

Towards a Fast and Robust MI-BCI: Online Adaptation of Stimulus Paradigm and Classification Model

Jiaxing Wang, Weiqun Wang, Jianqiang Su, Yihan Wang, and Zeng-Guang Hou, *Fellow, IEEE*

Abstract—Motor imagery based brain-computer interface (MI-BCI) has shown promising potential for improving motor function in neurorehabilitation and motor assistance among patients. However, the decoding accuracy of MI-BCI is limited by the non-stationarity and high inter-subject variability of electroencephalogram (EEG) signals. Moreover, decoding MI intention based on fixed-length EEG signals will not only increase the risk of misclassification but diminish the information transfer rate (ITR) of the BCI system. To overcome these limitations, an adaptive decoding method based on the synchronous adaptation of stimulus paradigm and classification model is proposed to realize a fast and robust MI-BCI. First, an attention-driven dynamic stopping strategy, which is designed based on the theta-beta ratio of EEG signals, is proposed to control the MI-related EEG acquisition time. It can adaptively minimize the data length used for classification under the ensurance of getting a credible classification result, thus improving brain-computer interaction efficiency. Then, the minimum distance to the Riemannian mean algorithm is introduced for the four-class EEG classification. To improve the classification accuracy, the classification model is adapted online based on the error-related potential to process the non-stationary characteristics of EEG signals. The feasibility of the proposed online collaborative optimization method in fast and accurate interaction was validated on ten healthy subjects. The results show that the proposed method can significantly improve the EEG classification accuracy by 2.73% with 9.04 ITR improvement compared with that without adaptation (paired t-test, $p < 0.05$). Moreover, MI duration of 2.57 seconds is recommended for stimulus paradigm design to achieve a better trade-off between accuracy and efficiency of brain-computer interaction. These phenomena further demonstrate the feasibility of the proposed method in advancing the development of MI-BCI with high efficiency, robustness, and flexibility.

Index Terms—Brain-computer interface, motor imagery duration, stimulus paradigm adjustment, classification model adaptation, information transfer rate.

This work is supported in part by the National Key R&D Program of China under Grant 2022YFC3601100; in part by the National Natural Science Foundation of China under Grants 62203440 and 62250058; and in part by the Beijing Natural Science Foundation under Grant L232021. (*Corresponding authors: Zeng-Guang Hou, Weiqun Wang*)

Jiaxing Wang, Weiqun Wang, Jianqiang Su and Yihan Wang are with the State Key Laboratory of Multimodal Artificial Intelligence Systems, Institute of Automation, Chinese Academy of Sciences, Beijing 100190, China (e-mail: jiaxing.wang@ia.ac.cn).

Zeng-Guang Hou is with the State Key Laboratory of Multimodal Artificial Intelligence Systems, Institute of Automation, Chinese Academy of Sciences, Beijing 100190, China, also with the School of Artificial Intelligence, University of Chinese Academy of Sciences, Beijing 100049, China, also with the CAS Center for Excellence in Brain Science and Intelligence Technology, Beijing 100190, China, and also with CASIA-MUST Joint Laboratory of Intelligence Science and Technology, Institute of Systems Engineering, Macau University of Science and Technology, Macao, China. (e-mail: zengguang.hou@ia.ac.cn).

I. INTRODUCTION

BRAIN-COMPUTER interface (BCI) has emerged as a promising technology to provide a new communication channel that is independent of the muscular and nervous systems [1]–[3]. BCI technology typically uses non-invasive methods to record electrical signals from the brain, such as electroencephalography (EEG), and then translate these signals into control commands for the device [4]–[6]. One type of BCI that has gained significant attention is the Motor Imagery Based Brain-Computer Interface (MI-BCI), which relies on the imagination of movement rather than actual movement to control the device [7], [8]. MI-BCI has shown great promise in various applications, including the development of assistive technology for individuals with paralysis, stroke, or other motor impairments [9]–[13], as well as for neurorehabilitation, cognitive training, and sports performance enhancement [14], [15].

Numerous methods have been proposed to enhance classification performance for MI-BCI. For example, denoising and feature extraction algorithms that aim to improve the signal-to-noise ratio and discriminability of MI patterns have been widely studied [16], [17]. Recently, deep learning methods that integrate signal preprocessing, feature extraction, and classification into an end-to-end single model, have shown superior performance and promising potential for classification accuracy improvement, particularly for large-scale EEG databases [18]–[20]. Despite these advancements, obtaining an MI-BCI system with high accuracy and robustness is still challenging due to the individual differences in brain activity and non-stationary factors such as fatigue and electrode displacement [21]. The aforementioned BCIs lack adaptability to the dynamic changes of brain activity, leading to a low control stability of the BCI system.

One promising approach to improve MI-BCI performance is through online updating of decoding models [22]–[24]. The brain decoding model is a critical component of the BCI system, as it translates EEG signals into actionable commands. However, the model can become less accurate over time due to changes in the user's neural patterns or environmental factors. Many studies have shown the effectiveness of online model updating in classification accuracy improvement [25], [26]. Mainstream model updating methods can be divided into three types: model updating based on iterative learning [27], [28], model updating based on decision value evaluation [29], [30], and model updating based on the error-related potential

(Errp) [31]. For example, in 2020, Ma *et al.* proposed an online learning method using projections onto shrinkage closed balls for adaptive BCI to improve the generalization of the classifier [27]. Similarly, an online model adaptation method using a recurrent adaptive neuro-fuzzy network was proposed, which improved the four-class classification accuracy by 7.8% [28].

However, most BCI systems only focus on classification model adaptation-based EEG decoding accuracy improvement, without taking the EEG acquisition part into account. Actually, decoding subjects' intentions by analyzing EEG signals with a fixed acquisition time, will not only heighten the likelihood of misclassification but significantly diminish the information transfer rate (ITR) of the BCI system. Therefore, in contrast to the fixed-stopping (FS) strategy, we prefer to determine the quality of the EEG features and check the classification confidence for each trial before stopping EEG collection. By automatically estimating the classification confidence, the dynamic stopping (DS) strategy could adaptively minimize the data length used for classification under the premise of ensuring classification accuracy, thus realizing system ITR improvement. Towards this topic, some works have introduced the concept of "quality of operator" (QoO) to achieve DS-based EEG acquisition. QoO is calculated based on sample entropy and power spectral density of EEG signals to indicate the classification confidence, and the acquisition time of EEG signals can be dynamically adjusted according to the confidence [32], [33]. In addition, Ming *et al.* proposed a Bayes estimation-based DS strategy to control the EEG signal acquisition time adaptively, thus realizing a high-speed BCI [34]–[36].

To realize a fast and robust MI-BCI system, both adaptive stimulus paradigm adjustment and decoding model updating are essential. To the best of our knowledge, the existing work on BCI performance improvement relies on either stimulus paradigm adaptation or decoding model updating. Since both factors are crucial in BCI systems, it is urgently necessary to investigate whether there is a conflict between stimulation paradigm adjustment and decoding model adaptation. Only by addressing this issue can we further enhance the performance of BCI system and ultimately advance the development of BCI technology.

Therefore, in this study, a synchronous optimization method based on the adaptation of both stimulus paradigm and classification model is proposed to achieve an MI-BCI system with high efficiency and accuracy. On one hand, in order to improve system ITR, an attention-driven DS strategy is proposed to adjust the MI duration online, thus controlling the acquisition time of required EEG signals. It can adaptively minimize the data length used for classification under the ensurance of getting a credible classification result, thus improving brain-computer interaction efficiency. On the other hand, in order to improve the brain decoding accuracy, an Errp-based adaptive classification model updating method is introduced to overcome the non-stationary characteristics of EEG signals. Online adaptation allows the system learns from new data and updates the classification model continuously. Therefore, it can better distinguish between different EEG patterns and provide a more accurate classification online. Ten healthy subjects were

recruited to validate the feasibility of the proposed system. The results show that our methods can improve the classification accuracy by 2.73% significantly with 9.04 ITR improvement compared with the method without adaptation. In addition, MI duration lasting 2.57 seconds is recommended for stimulus paradigm design to achieve a better trade-off between accuracy and efficiency of brain-computer interaction.

The main contributions of our work are given as follows:

- 1) An attention-driven DS strategy, which can dynamically adjust the MI-related EEG acquisition time, is proposed to minimize the data length used for classification under the ensurance of getting a credible classification result, thus improving the ITR of the BCI system.
- 2) An Errp-based online decoding model adaptation method, which can enhance the adaptability of the system to the brain status variation, is proposed to improve long-term classification performance.
- 3) The feasibility of the proposed synchronous adaptation method was verified on 10 subjects, which demonstrated a significant improvement in classification accuracy and system ITR.

The remainder of this paper is structured as follows. Section II introduced the proposed adaptive MI-BCI system and the detailed adaptation methods are given in Section III. The experiment design and analysis results are presented in Sections IV and V, respectively. Finally, the discussion and conclusion are given in Sections VI and VII.

II. OVERALL SYSTEM

An adaptive MI-BCI system based on online paradigm adjustment and classification model updating is designed in this study to realize a fast and robust MI-BCI. The whole system mainly consists of four parts, which are the stimulus paradigm presentation module, the EEG acquisition and processing module, the MI intention classification module, and the adaptation control center, as shown in Fig. 1.

Specifically, the stimulus paradigm presentation module is designed as a four-class MI task. The participants are supposed to perform different MI tasks according to the cues displayed on the computer. During the experiment, subjects' brain activities are collected and analyzed in real time by the EEG acquisition and processing module. Finally, their MI intention, which is decoded by the EEG classification module, will be obtained and displayed on the screen. In addition, the MI duration and the decoding model are updated by the adaptation control center to improve the performance of the MI-BCI system in efficiency and accuracy.

A. Stimulus Paradigm Design

Four different MI tasks are included in the cue-based MI-BCI paradigm: imagining the movement of the left hand, right hand, tongue, and both feet. Two sessions named off-line session and on-line session conducted on different days were designed for each subject. The paradigm is illustrated in Fig. 2. During the experiment, subjects were seated in a comfortable armchair facing a screen. Each trial began with a fixation cross displayed on the screen at $t = 0s$. After one second ($t = 1s$),

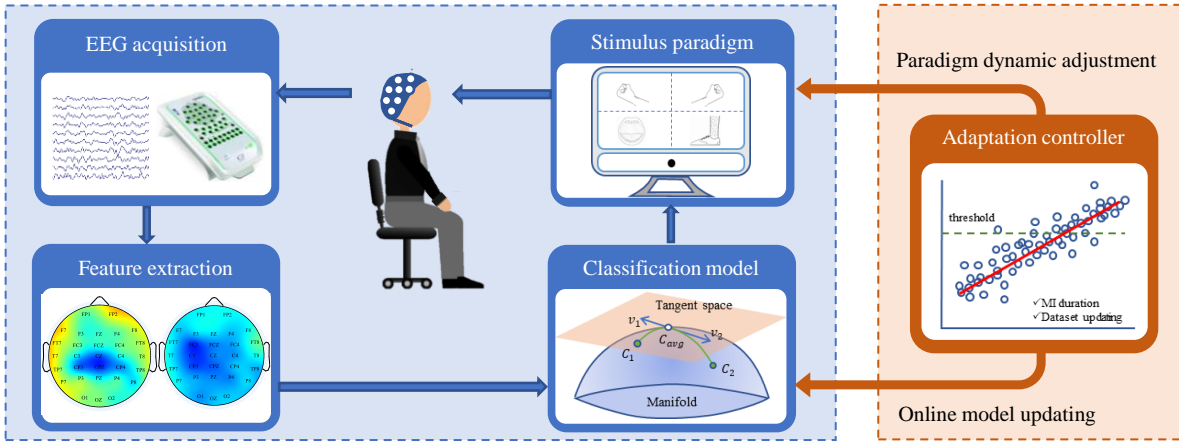


Fig. 1. The constitution of the proposed adaptive MI-BCI system.

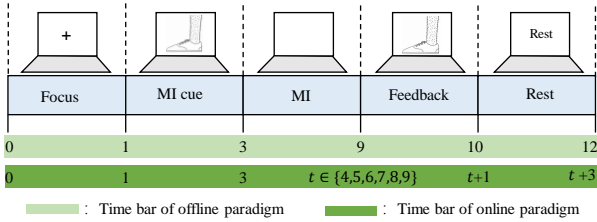


Fig. 2. Timing scheme of the paradigm.

an animation indicating one of the four classes (left hand, right hand, tongue, or feet) appeared and remained on the screen for 2s. This animation served as a cue for the subjects to engage in the corresponding MI task for the subsequent 6s. Specifically, after the MI cue disappeared, the subjects were instructed to perform the corresponding MI task until a feedback animation appeared. During the feedback stage, the subjects were required to mentally evaluate the consistency between the feedback signal and their actual MI task. Finally, a brief 2s break was provided.

The timing scheme of the online paradigm differs from the offline paradigm, primarily in terms of the duration of MI. In the offline experiment, the MI duration is fixed at 6s. However, in the online experiment, the MI duration is dynamically adjusted from 1s to 6s based on the proposed attention-driven DS strategy to enhance the system ITR.

B. Classification Algorithm

EEG signals are complex, high-dimensional data that exhibit non-Euclidean properties. Traditional signal processing methods are not sufficient to fully capture the underlying neural processes. Riemannian geometry provides a powerful framework for analyzing EEG data by allowing for the analysis of covariance matrices, which capture the statistical information between EEG signals, rather than the raw EEG signals themselves. Therefore, Riemannian manifolds are less sensitive to noise and artifacts than traditional machine learning-based methods. They are more easily adaptable to new EEG signals, as they do not rely on specific features or patterns of

activity that may be unique to a particular data. This makes them more generalizable and potentially more useful in clinical settings [37], [38].

We employed Riemannian geometry to analyze the multi-class EEG signals. Let X_i represents a short segment of the required EEG signals, and X_i can be denoted as follows:

$$X_i = [X_i^{T_i}, \dots, X_i^{T_i+T_s-1}] \in \mathbb{R}^{n \times T_s} \quad (1)$$

where X_i corresponds to the i th trail of imaged movement starting at time $t = T_i$. T_s denotes the number of sampled points of the selected segment, n is the number of channels.

For the i th trail, the spatial covariance matrix (SCM) $P_i \in \mathbb{R}^{n \times n}$ can be calculated as follows:

$$P_i = \frac{1}{T_s - 1} X_i X_i^T \quad (2)$$

In order to leverage the intrinsic information of SCM, which resides in the symmetric and positive definite (SPD) space, we assign a Riemannian distance to it. The Riemannian distance between two SPD matrices, denoted as P_1 and P_2 , within the space of $P(n)$, can be defined as follows [39]:

$$\Theta_R(P_1, P_2) = \|\log(P_1^{-1}P_2)\|_F = \left[\sum_{i=1}^n \log^2 \lambda_i \right]^{\frac{1}{2}} \quad (3)$$

where $\lambda_i (i = 1, \dots, n)$ are the real eigenvalues of $P_1^{-1}P_2$.

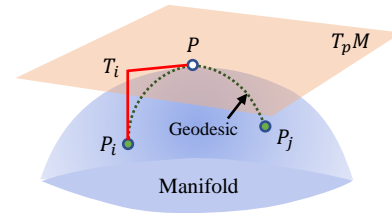


Fig. 3. The diagram of Riemannian manifold. P_i, P_j are two points in Riemannian manifold. The tangent space $T_C M$ is associated with the point P . Dotted line between P_i and P is the geodesic. The corresponding point of P_i on the tangent space is denoted as T_i . These points can be converted to each other using exponential mapping and logarithmic mapping.

The space of SPD matrices, defined by the Riemannian

distance, is referred to Riemannian manifold. The manifold is a topological space with local Euclidean space. Fig. 3 illustrates the Riemannian manifold along with its tangent space. The $T_p M$ is a tangent space based on the Riemannian mean. The SCM in the Riemannian manifold can be transformed to the tangent space using the logarithmic mapping (Eq. (4)), and conversely, it can be restored to the manifold using the exponential mapping (Eq. (5)) [37].

$$\log_P(P_i) = T_i = P^{-\frac{1}{2}} \log(P^{-\frac{1}{2}} P_i P^{-\frac{1}{2}}) P^{\frac{1}{2}} \quad (4)$$

$$\exp_P(T_i) = P_i = P^{\frac{1}{2}} \exp(P^{-\frac{1}{2}} T_i P^{-\frac{1}{2}}) P^{\frac{1}{2}} \quad (5)$$

Given m SPD matrices P_1, \dots, P_m , the geometric mean in the Riemannian sense is defined as:

$$\Theta(P_1, \dots, P_m) = \arg \min_{P \in P(n)} \sum_{i=1}^m \delta_R^2(P, P_i) \quad (6)$$

Filter Geodesic Minimum Distance to Riemannian Mean (FGMDRM), which is a distance-based classifier that computes the geodesic distance between the Riemannian mean of the training data and the test data, is introduced to classify MI tasks. Specifically, we first compute the Riemannian mean of the covariance matrices for each class by Eq. (3). Then, the geodesic distances between the Riemannian mean of each class and the individual covariance matrices can be calculated by Eq. (6). Finally, Fisher's discriminant analysis to the geodesic distances is applied to obtain a discriminant function that maximally separates the classes. For the test covariance matrix P_t , the aforementioned discriminant function will be introduced to classify the new EEG signals based on their geodesic distances to the Riemannian mean of each class.

III. ADAPTATION METHODS

A. Attention-Driven Stimulus Paradigm Adjustment

Subjects' attention level on the MI task is a crucial factor in the quality of acquired EEG signals. Therefore, their attention states are monitored throughout the experiment to determine the MI duration. When the attention state is good, the MI duration can be shortened to improve the system ITR while ensuring accurate EEG classification. Conversely, the duration is restored to prioritize the accurate decoding of motor intention.

The theta to beta EEG power ratio (TBR) [40], [41], based on the international 10–20 system (Fig. 4), was introduced to calculate subjects' attention states. Our previous work [42] has demonstrated that EEG signals acquired from frontal and temporal regions are most relevant to the subjects' attention states. Considering that EEG signals collected by the outer electrodes are easily contaminated by muscle artifacts, only F3, Fz, and F4 channels are selected for the final TBR-based attention calculation.

Before the attention calculation, a Butterworth bandpass filter (0.5-30 Hz) is applied to the raw EEG signals to filter out noise. Then the energy of theta (3-8 Hz) and beta (12-30 Hz) bands can be calculated by fast Fourier transform, respectively

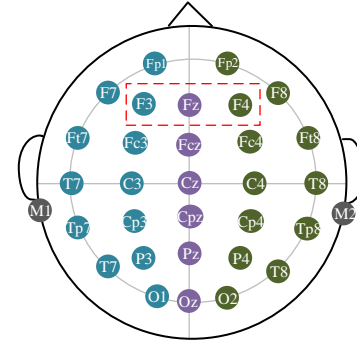


Fig. 4. International 10–20 system for 32-channel EEG cap, where F3, Fz, and F4 are the electrodes used for TBR calculation.

($E(\theta)$ and $E(\beta)$). Finally, subjects' attention at time t can be calculated as follows:

$$T_E(t) = \sum_{c=1}^3 \frac{E_c(\theta)}{E_c(\beta)} \quad (7)$$

where c represents the channel index. With the increase of $T_E(t)$, the subject attention paid to the experiment is decreased correspondingly.

Subjects' attention is only monitored during the "MI" stage based on the Algorithm 1. Specifically, during the MI stage,

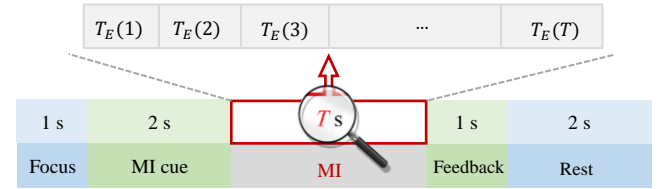


Fig. 5. MI duration adjustment of the stimulus paradigm. The MI duration T is varied according to subjects' real-time attention states.

$T_E(t)$ is calculated based on the latest one-second EEG signals, and it is updated per second. Considering the non-stationarity of EEG signals, the cumulative mean attention level $C_{tbr}(t)$, rather than the one-second attention level $T_E(t)$, is used to indicate subjects' attention states.

$$C_{tbr}(t) = \frac{\sum_{j=1}^t T_E(j)}{t} \quad (8)$$

During the online MI experiment, if $C_{tbr}(t)$ is lower than the threshold, which represents a high attention state, the "MI" stage will be stopped correspondingly, thus minimizing the data length used for classification under the ensurance of getting a credible classification. Subjects' psychological and physiological state fluctuates all the time, which makes the attention threshold difficult to be determined. To overcome this issue, the attention threshold is dynamically updated based on the mean value of $T_E(t)$ obtained during the latest five trials, rather than being set to a fixed value.

B. Errp-based MI Classifier Adaptation

Classification model adaptation can improve the adaptability of the BCI system to changes in brain states, thereby reducing

Algorithm 1 Attention-driven stimulus paradigm adjustment algorithm

- 1: T : MI duration of each EEG trial, initialized algorithm 6 seconds (the maximum MI duration).
- 2: $t \in \mathbb{N}^+$: duration of EEG data has been obtained during the MI phase, initialized to 0.
- 3: $c \in \{1, 2, 3\}$: EEC channel index used for attention calculation.
- 4: $E(\theta)$: theta energy calculated based on the latest one-second EEG signals.
- 5: $E(\beta)$: beta energy calculated based on the latest one-second EEG signals.
- 6: $T_E(t)$: theta to beta ratio based attention level at time t .
- 7: $C_{tbr}(t)$: cumulative mean attention level at time t .
- 8: $C_{threshold}$: threshold of attention level, which is updated online based on the mean value of $T_E(t)$ obtained during the latest five trials.
- 9: **for** each MI duration **do**
- 10: **do**
- 11: $t = t + 1$;
- 12: Compute $T_E(t)$ with $E_c(\theta)$ and $E_c(\beta)$ using Eq.(7).
- 13: Compute $C_{tbr}(t)$ with $T_E(t)$ obtained in the latest t seconds using Eq. (8).
- 14: **while** $C_{tbr}(t) \geq C_{threshold}$ & $t < T$
- 15: Stop MI stage at time t ;
- 16: Update $C_{threshold}$ based on the mean value of $T_E(t)$ obtained during the latest five trials.
- 17: Initialize t to 0.
- 18: **end for**

the calibration time of BCI and improving the online performance in accuracy and robustness.

ErrP refers to event-related potentials in the brain that are generated as a response to errors [43]. Previous works have demonstrated that ErrP can be classified with sufficient accuracy [43], [44]. In this study, ErrP is utilized for classification model adaptation, which refers to gradually updating the classification model as data arrives, based on the user's ErrP response to BCI feedback results.

Errp Detection. EEG signals, acquired from 300 ms to 900 ms after the feedback given, were used for Errp classifier training and recognition [45]. The common spatial pattern (CSP) and support vector machine (SVM) are adopted for feature extraction and classification. EEG signal frequency is a key factor affecting the performance of CSP. Considering that ErrP is mainly composed of mu and theta rhythms, which dominates in the low-frequency range, only 1-16 Hz EEG signals are used for CSP-based feature extraction. The goal of CSP is to find a spatial filter $W \in \mathbb{R}^{M \times M}$ (M denotes the channel number of the acquired EEG), by which the

discrimination between two patterns can be maximized. The optimal spatial filter W can be calculated by maximizing the following equation:

$$J(W) = \frac{W^T C_1 W}{W^T C_2 W} \quad (9)$$

where C_i denotes the mean of all sample covariance matrices of each class. Here, EEG is divided into two classes, S_1 and S_2 that denote EEG signals with Errp or without Errp, respectively. Once the optimal spatial filter is obtained, the most discrimination vector between S_1 and S_2 can be obtained by Eq. (10).

$$F(i) = \frac{\text{var}(W S_i)}{\text{var}(W S_1) + \text{var}(W S_2)} \quad (10)$$

where $F(i)$ and $\text{var}(\cdot)$ represent the feature and variance matrices of the i th-class EEG signals, respectively. The feature vector of each sample extracted by the CSP based on the Fz, Fcz, Cz, Cpz, and Pz channels is normalized to the range of -1 to 1, and serves as the input of the SVM to establish the Errp detection model [45].

MI Classifier Adaptation. To further improve classification performance after offline model training and calibration, the classifier is adapted online in an unsupervised manner. Specifically, as shown in Fig. 6, during the online experiment,

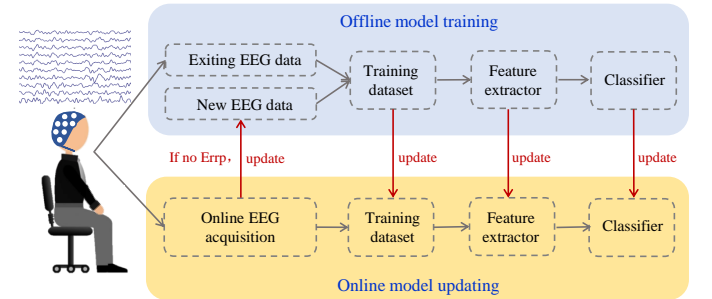


Fig. 6. Flow diagram of online classifier adaptation.

if an ErrP is detected, the data will be excluded from the classifier's adaptation process because the estimated class label is suspected to be wrong and the true label is unknown. Conversely, if no ErrP is detected, the MI data obtained will be utilized for adaptation in an unsupervised manner. More concretely, for a new trial T , which is classified as label L , if no ErrP is detected, L will be deemed as the correct class label, and the classifier will be adapted by adding (T, L) to the training data, followed by retraining the classifier.

The adaptation of the classifier occurs concurrently with the EEG processing and classification. These modules communicate with each other through shared memory. The model update is a microsecond scale. In case of new EEG data arriving while the adaptation is in progress, it is stored in a buffer and utilized for the next iteration of the adaptation loop.

IV. EXPERIMENT

To assess the feasibility of the proposed method in improving brain decoding accuracy and system ITR, a con-

trast experiment was designed based on whether the online adaptation of the paradigm and classifier was used or not. Before the contrast experiment, an offline experiment was conducted firstly to collect training data for the personalized MI classifier and Errp classifier establishment, respectively. During the online training, the paradigm parameters were set up to be the same as the offline for the control group (CG), whose MI duration was fixed to 6s, and the MI classifier was antique, instead of updating online. For the experiment group (EG), the MI duration of the stimulus paradigm was adjusted online to optimize the acquisition duration of MI-related EEG signals. Moreover, the MI classifier was updated in real-time to adapt to the time-varying characteristics of EEG depending on whether Errp was detected.

The offline session and the online session were conducted on different days. In addition, to establish the Errp classifier, the proportion of error stimuli was controlled at around 20% during the offline experiment to ensure the effectiveness of the experiment, thus obtaining Errp signals with high quality and stability.

Ten healthy subjects, comprising an equal number of males and females with ages ranging from 21 to 35 years (mean 24 ± 1.6 years) participated in the experiments. All participants had no history of neurological problems or prior experience with MI to minimize potential confounding factors. Moreover, the participants were required to demonstrate the capability to comprehend and independently execute the MI-BCI experiment, ensuring the effectiveness of the experimental results. The study was approved by the ethics committee of the Institute of Automation, Chinese Academy of Sciences (approval number: IA21-2211-06, date of approval: November 9, 2022). Written consent was obtained from all subjects after providing them with detailed information about the experiment. Each subject participated in both CG and EG experiments. The order of the two experiments was randomized to increase the internal validity of the experiment by reducing potential sources of interference.

During the experiment, subjects were seated in a wheelchair and instructed to engage in MI tasks involving the left hand, right hand, tongue, and feet, respectively, based on the provided cues (refer to Fig. 1). EEG data was recorded using a 32-channel NeuroScan system at a sampling rate of 256Hz. The ground electrode is located at Afz and the reference electrode located between Cz and CPz. The common average reference (CAR) [46], which can reduce the impact of common mode noise and improve signal spatial resolution, was adopted as the reference method in this study. Previous studies have demonstrated a strong correlation between EEG signals in the low-frequency band (8-30Hz) and brain activity of MI [47]. Therefore, in this study, the raw EEG signals were filtered using a bandpass filter set at 8-30Hz to focus on the relevant frequency range. To increase the number of training samples for MI classifier, cropped training strategy with a 2-second-long sliding window was adopted to train the classifier. Mean classification probability was calculated to determine the trials' final classification results if the participants' MI duration for each trial was longer than 2s.

V. CLASSIFICATION RESULTS

The classification accuracy, as well as the system ITR, were introduced to compare the MI-BCI performance under different methods. Specifically, ITR can be computed with the following equation:

$$ITR = \frac{60}{T} (\log_2(M) + p \log_2(p) + (1-p) \log_2 \frac{1-p}{M-1}) \quad (11)$$

where T denotes the MI duration, M denotes the number of classes, and p denotes the classification accuracy. The MI classifier performance trained by EEG signals with different time lengths was first calculated and given in the offline analysis section, followed by which the online experiment results with different adaptation methods were detailed.

A. Offline Experiment Analysis

In the offline classification experiment, each subject completed a total of 6 runs, with short breaks in between. Each run comprised 24 trials, consisting of 6 trials for each of the four possible classes, thus yielding a total of 144 trials. The timing of the paradigm is shown in Fig. 2, whose MI duration is 6s. We separately intercepted MI-stage EEG signals with time lengths of 1s, 2s, 3s, 4s, 5s, and 6s after the cue disappeared, and used Riemannian-based FGMDRM algorithm for classification under different MI duration. For the convenience of subsequent description, C_n is defined as the classifier corresponding to the MI duration lasting n seconds. Specifically, for the training of classifiers C_3 , C_4 , C_5 , and C_6 , we first increased the number of samples through overlapped time slice strategy with 2s window length and 1s step size. The final classification result corresponding to each trial was decided by the max-mean classification probability. Subject-specific classification accuracy and the mean classification accuracy for EEG signals under different MI duration are shown in Fig. 7.

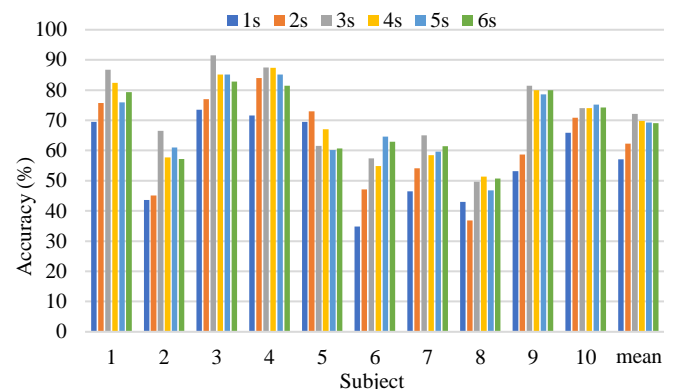


Fig. 7. Subject-specific classification accuracy and the mean classification accuracy for EEG signals under different MI duration in the offline experiment.

Fig. 7 shows that the classification accuracy varies greatly among subjects, and different MI duration of the same subject will also cause the fluctuation of classification accuracy significantly. Subject 3 under 3s MI duration obtained the highest classification accuracy, and subject 6 under 1s MI duration

obtained the lowest accuracy. In general, for each subject, the classification accuracy first increased with the increase of MI duration and then remained or slightly decreased. It can be seen from the mean classification results that 3s MI duration led to the highest classification accuracy in the offline experiment. The reason for the decreased classification accuracy after 3s may be that long MI leads to decreased concentration of the imagery task and poorer quality of the acquired EEG signals, which lead to decreased accuracy.

B. Online Experiment Analysis

To validate the feasibility of the proposed method in online decoding performance improvement, four online experiments named “No adaptation”, “Model adaptation”, “MI duration adaptation” and “Both adaptation” were designed. Specifically, for Experiment #1-“No adaptation”, the MI duration was set to fixed-value integers of 1s to 6s, and the corresponding classification model was the offline training model without any adjustment. For the Experiment #2-“Model adaptation”, the classification model parameters were updated adaptively based on the aforementioned Errp-based MI classifier adaptation method. Similarly, the MI duration was adjusted online for the Experiment #3-“MI duration adaptation”. In Experiment #4-“Both adaptation”, both MI duration and classification model were updated simultaneously to improve the performance of the online BCI system further.

First of all, subject-specific classification accuracy and the mean classification accuracy in Experiment #1 without any online adaptation are shown in Fig. 8. It can be seen that there was a positive correlation between classification accuracy and MI duration. Compared with the offline experiment, the classification accuracy of Experiment #1 showed a significant decrease. The main reason leading to the reduction of classification accuracy is the non-stationarity characteristic of EEG since the offline experiment and the online experiment were carried out on two different days. This phenomenon further illustrates the importance of developing an adaptive BCI system.

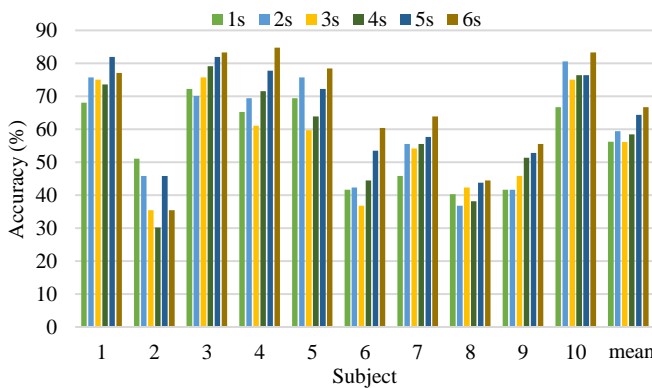


Fig. 8. Experiment #1: Subject-specific classification accuracy and the mean classification accuracy based on the method without any online adaptation.

In Experiment #2, the classification model was updated online to improve the classification performance, and the classification results are given in Fig. 9. The model adaptation

method was based on the Errp classification results, and the mean Errp classification accuracy was 92.1%. Fig. 9 shows that through online updating of the model, the classification accuracy is significantly improved and 2.76% higher than that of offline classification. Online model updating can not only overcome the non-stationarity characteristic of EEG, but also increase the size of the training set by adding online EEG data, thus further improving the accuracy.

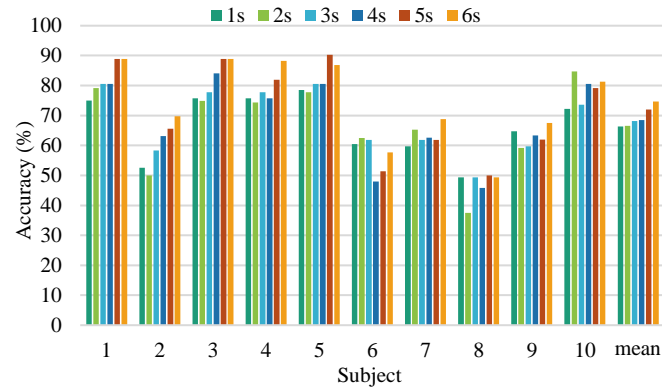


Fig. 9. Experiment #2: Subject-specific classification accuracy and the mean classification accuracy based on the method with online model adaptation.

Parallel to the improvement of classification accuracy, the MI duration was also adjusted online to improve ITR. The influence of online MI duration adjustment on classification accuracy is given in Fig. 10. It can be seen that the average MI duration of each subject was about 2.5s, which was significantly lower than 6s. However, the reduction of MI duration also leads to the reduction of classification accuracy. Fig. 10 also shows that individuals with high decoding accuracy, such as subjects 1, 3, 4, 5, and 10, required shorter MI duration compared to the others. This phenomenon demonstrated that some individuals have strong MI ability, thus high classification accuracy can be obtained even if the MI duration is reduced.

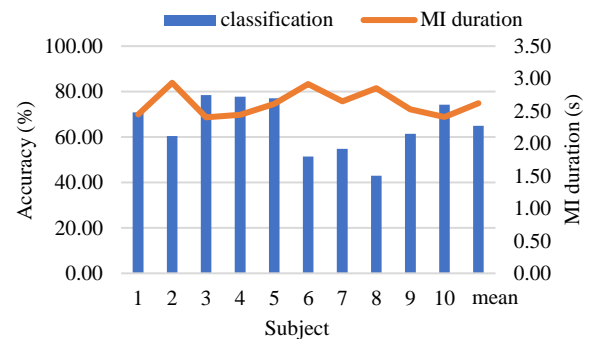


Fig. 10. Experiment #3: Classification accuracy and the mean MI duration for each subject by adaptive MI duration adjustment.

Finally, the classification accuracy and the mean MI duration for each subject with both model adaptation and MI duration adjustment are shown in Fig. 11. It can be seen that the model adaptation method improved the classification accuracy significantly compared to Fig. 10, but there was

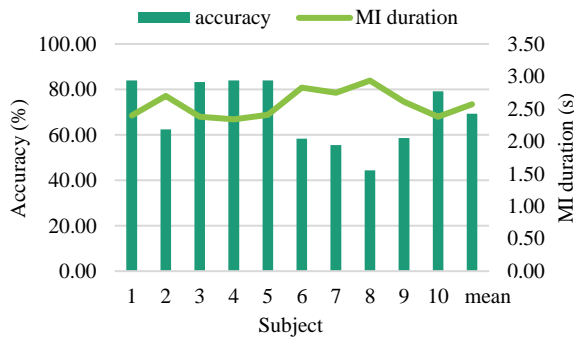


Fig. 11. Experiment #4: Classification accuracy and the mean MI duration for each subject with model adaptation and MI duration adjustment.

only a slight fluctuation in MI duration. In order to clearly compare the effects of different methods on the online MI-BCI performance, the classification accuracy, MI duration, and ITR under different methods are plotted together in Fig. 12. For

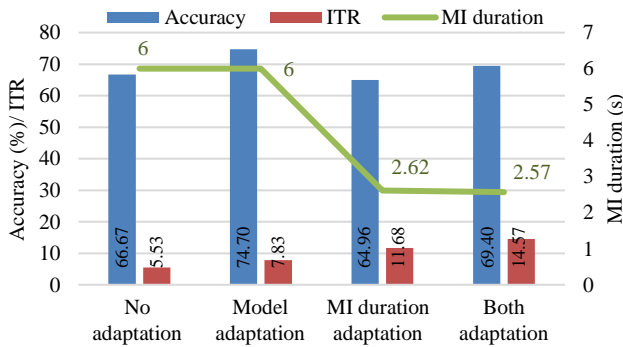


Fig. 12. Comparison of the effects of different methods on the MI-BCI performance in terms of classification accuracy, MI duration, and ITR.

the method without adaptation that was tested in Experiment #1, the mean classification accuracy (66.67%) under 6s MI duration was selected for the final comparison, since the classification accuracy under 1s to 5s MI duration was all lower than 66.67% (Fig. 8). Similarly, for the method with model adaptation (Experiment #2), the mean classification accuracy (74.70%) under 6s MI duration was selected for the final comparison. Further, the paired t-test method was used to analyze the statistical difference of model performance between different experiments.

For classification accuracy performance, Fig. 12 shows that the model adaptation method achieved the highest accuracy (74.7%) compared to the others (Experiment #2 vs #1: $p = 0.0384 < 0.05$; Experiment #2 vs #3: $p = 0 < 0.05$; Experiment #2 vs #4: $p = 0.0018 < 0.05$), but the corresponding MI duration is also the highest (6s). Considering that ITR is also an important index to characterize the BCI system, ITR is also calculated using Eq. (11). The key factors affecting ITR mainly include classification accuracy and MI duration. Fig. 12 shows that the model adaptation method can improve ITR significantly by improving classification accuracy (Experiment #2 vs #1: $p = 0.0137 < 0.05$), and MI duration adaptation method allows for an improvement of ITR by reducing the MI duration (Experiment #3 vs #1: $p = 0.0006 < 0.05$). Therefore, the pro-

posed method of online adaptation of both stimulus paradigm and classification model realized the highest ITR (Experiment #4 vs #1: $p = 0.0012 < 0.05$). The cost of the improvement of ITR is the reduction of classification accuracy compared to the method with only model adaptation. According to the performance of “Both adaptation”, the MI duration of 2.57 seconds is recommended for stimulus paradigm design to achieve a better trade-off between the accuracy and efficiency of BCI, and we can fine-tune the MI duration time according to different demands to realize a customized BCI system.

The confusion matrices of the online classification accuracy for different strategies are given in Fig. 13, where “T”, “F”, “L”, and “R” denote the categories named tongue, feet, left hand, and right hand, respectively. On one hand, the common phenomenon is that for different methods, tongue and foot MI are easily misclassified into another category, and similarly, left and right hand MI are easily misclassified into another category. For example, in subfigure 4, the probability of tongue MI being misclassified as foot MI is as high as 0.15, which is the same as the probability of foot MI being misclassified as tongue MI. Meanwhile, the probability that the left-hand MI is misclassified as the right hand reached 0.17. On the other hand, compared with the method without adaptation, the model updating method mainly improved the decoding accuracy in tongue and left-hand MI. In particular, model updating can correct part of left-hand MI that was misclassified as right-hand MI by method without adaptation.

The visualization of MI duration for each class under different methods is shown in Fig. 14. From the results, it can be seen that due to the difficulty in classifying the left-hand MI (low classification accuracy in left hand, Fig. 13), the MI duration needed for the classification of left-hand MI was longer than the other categories. Moreover, the MI duration for left-hand classification using the method with both adaptations is significantly lower than that under the method with only MI duration adaptation ($p = 0.02 < 0.05$).

In order to compare the characteristics of brain activities under different MI tasks, the PSD was calculated for each EEG channel except for the channels of M1 and M2. Specifically, the EEG signals of all trials for each subject were averaged separately. Then, the PSDs of the EEG data corresponding to the MI state ($t=3-9s$) and the cue state ($t=1-3s$) were calculated, respectively. The relative PSDs for the band of 8-12 Hz were computed by subtraction. The topographical distribution of averaged alpha band power (ERD and ERS in 8 to 12 Hz) during four MI tasks are given in Fig. 15. Data are displayed from 2 representative subjects of #2 and #5.

It can be seen from Fig. 15 that a significant ERD around electrodes C3 and C4 with contralateral dominance can be found during right and left hand MI, respectively. Quite different patterns are found with foot and tongue MI. The representation of the foot in the cerebral cortex is in the mesial wall. A midcentral mu ERD was found in the majority of subjects. However, it is intriguing to note that both the feet and tongue MI elicited enhancement in the mu rhythm (mu ERS) within the hand area for certain subjects, exemplified by Subject #5. This concurrent manifestation of ERD and ERS provides a compelling illustration of the “focal ERD/surround

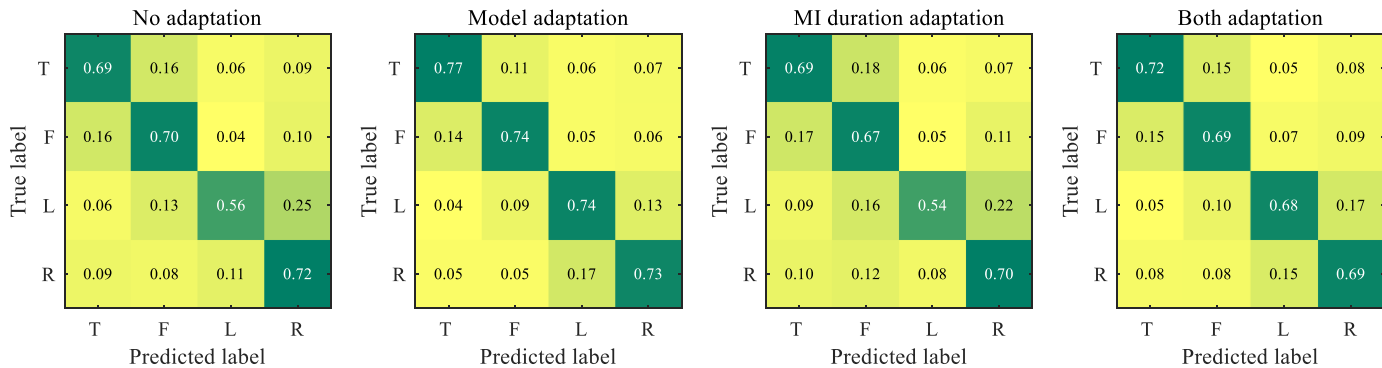


Fig. 13. Flow diagram of online classifier adaptation.

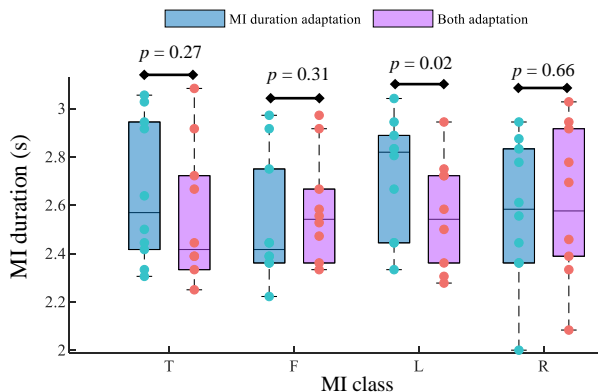


Fig. 14. The box and scatter plots of the mean MI duration for different methods.

ERS” phenomenon, which captures the observation that the desynchronization of the alpha (μ) rhythm does not occur in isolation but is accompanied by an augmentation of synchronization in adjacent cortical regions associated with the same or another modality [48], [49].

To demonstrate the superiority of the proposed synchronous optimization method, many classical algorithms and the latest methods in the field of EEG-based MI-BCIs were compared. Table I shows that compared with the traditional methods, the proposed method achieved the highest performance in both classification accuracy and ITR. When compared with the deep learning-based methods, our method maintains the highest ITR despite a slightly lower accuracy compared to Deep ConvNet, which demonstrated the superiority of the proposed method.

VI. DISCUSSION

Compared with the traditional MI-BCI system, the proposed synchronous optimization method based on the online adaptation of both stimulus paradigm and classification model improved not only classification accuracy but also system ITR. Moreover, it obtained the best performance compared with BCI systems with only online model adaptation or online stimulus paradigm adjustment. This phenomenon demonstrated that there is no conflict between the optimization of the stimulation paradigm and the decoding model, thus the perfor-

TABLE I
COMPARISON OF MODEL PERFORMANCE IN CLASSIFICATION ACCURACY AND SYSTEM ITR BETWEEN THE PROPOSED METHOD AND EXISTING MODELS.

Method Category	Paper	Method	Acc	ITR
Traditional Method	Ours	/	0.69	14.57
	[50]	CSP+LDA	0.56	6.26
Traditional Method	[51]	MRA+LDA	0.59	7.47
	[51]	CSP+SVM	0.60	7.90
	[52]	FBCSP+SVM	0.68	11.77
Deep learning based method	[53]	EEGNet	0.66	10.73
	[54]	Deep ConvNet	0.70	12.86
	[55]	SYAN	0.66	10.73
	[56]	MIN2Net	0.65	10.22

mance of MI-BCI can be further improved by the synchronous optimization of these two aspects.

For the adjustment of the stimulus paradigm, the commonly used strategy is a fixed duration for each stimulation, in which the acquired MI-related EEG data length is fixed. Generally speaking, the EEG features will be more stable with the increase of the MI-related EEG data length. However, long-time MI would lead to subjects’ over-fatigue or under-utilization of the MI technique. Another is the online MI duration adjustment method based on subjects’ task performance or physiological status. It can analyze the quality of the EEG features and check the classification confidence for each trial before stopping EEG collection. In this paper, subjects’ EEG-based attention level was introduced to guide the adjustment of the MI duration online. The adaptive determination of the output time for each individual trial allowed for a significant improvement in system ITR without compromising the classification accuracy. This method relies on accurate and consistent measures of subjects’ mental states, and the main drawback of MI duration adjustment methods is that they rely on certain assumptions (such as stop threshold) and may not always accurately reflect the participant’s needs or abilities, which could limit their practicality for widespread use.

The proposed online model adaptation method is based on

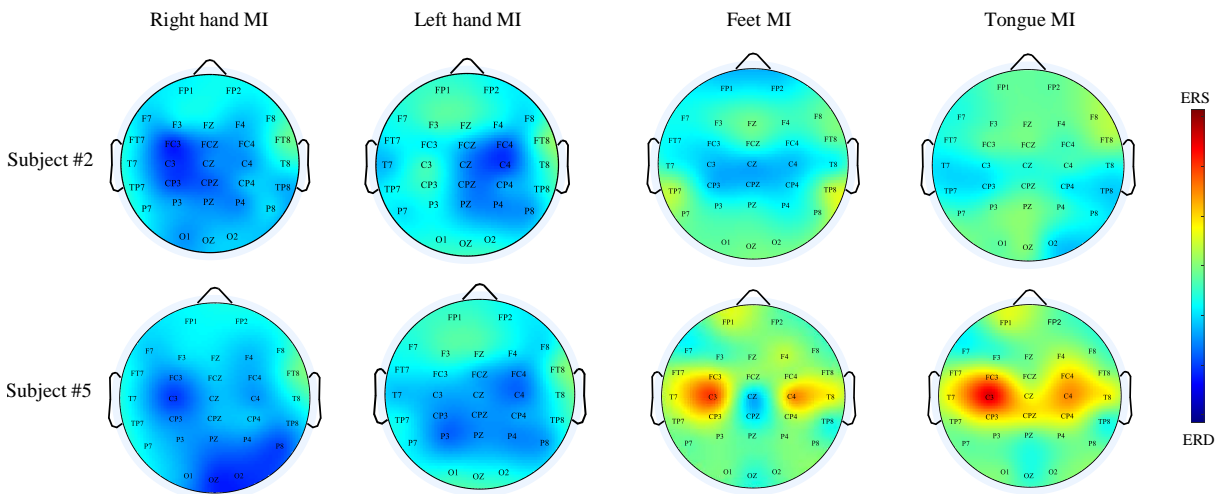


Fig. 15. Brain topologies (ERD, ERS) in the alpha band during four MI tasks based on the “both adaptation” method. Data are displayed from 2 representative subjects. “Blue” indicates ERD and “Red” indicates ERS.

ErrP, which can be detected with a sufficient average accuracy of 92.1% in this paper. To guarantee the ErrP-based online model adaptation performance, it is essential to maintain participants’ high concentration throughout the experimental process, which ensures accurate induction of ErrP signals, guiding the effective selection of MI data used for model adaptation. Additionally, the MI-BCI experiment designed in this study is an online experiment. The MI duration in each trial varies according to subjects’ real-time attention states. The MI classification results and ErrP signals triggered by different MI durations will vary, and thus the proposed method cannot be validated using publicly available offline datasets, as the experiment requires the subjects’ real-time participation.

Although online MI-BCIs have great potential in the field of neurorehabilitation, there are still several technological challenges and limitations that need to be addressed. Here are some of the technical bottlenecks of EEG-based MI-BCIs in neurorehabilitation, which can guide the development of BCIs. One of the main technical bottlenecks of online MI-BCIs is the quality of the signals obtained from the brain. The signals are often weak and noisy, which can lead to inaccurate or inconsistent decoding of motor intentions. Another challenge is the time and effort required to train users to control the BCI effectively. It can take a significant amount of time and practice for users to learn how to modulate their brain signals in a consistent and accurate way. In addition, there is a high degree of individual variability in how people generate and modulate their MI signals. This variability can make it difficult to develop BCI systems that work effectively for all users. Moreover, BCIs need to be adaptable to changes in the user’s mental and physical state. For example, changes in fatigue or attention can affect the quality of the brain signals, which can affect the performance of the BCI. To overcome these challenges, potential solutions and future directions involve advancements in signal processing techniques to mitigate noise, personalized MI-BCI paradigm to expedite user learning, and the integration of deep learning algorithms

for individualized MI signal decoding. Additionally, exploring novel technologies such as virtual reality or gamification can enhance user engagement and accelerate the learning process. Besides, the effectiveness of the proposed method in improving the decoding accuracy and efficiency of MI-BCI system for healthy individuals was verified in this study. In the future, conducting clinical experiments is necessary to validate the feasibility and effectiveness of the proposed method in real-world clinical applications.

VII. CONCLUSION

In this study, a fast and robust MI-BCI system based on the online adaptation of the stimulus paradigm and classification model was proposed to help subjects perform MI effectively. The performance of the proposed adaptive MI-BCI was validated through the comparison experiments on ten subjects. The experiment results showed that the classification accuracy was significantly improved ($p < 0.05$) by using the proposed adaptive MI-BCI system; meanwhile, the system ITR can be further improved to enhance the usefulness of BCI systems. In future work, on the one hand, we should improve the effectiveness of the classification algorithm, especially in cross-subject classification, and explore various characteristic metrics of users, not just attention level; on the other hand, the proposed MI-BCI will be combined with the rehabilitation robot to provide effective rehabilitation strategies in the future.

REFERENCES

- [1] M. F. Mridha, S. C. Das, M. M. Kabir, A. A. Lima, M. R. Islam, and Y. Watanobe, “Brain-computer interface: Advancement and challenges,” *Sensors*, vol. 21, no. 17, p. 5746, 2021.
- [2] R. Mane, T. Chouhan, and C. Guan, “BCI for stroke rehabilitation: motor and beyond,” *Journal of Neural Engineering*, vol. 17, no. 4, p. 041001, 2020.
- [3] P. Arpaia, N. Moccaldi, R. Prevete, I. Sannino, and A. Tedesco, “A wearable EEG instrument for real-time frontal asymmetry monitoring in worker stress analysis,” *IEEE Transactions on Instrumentation and Measurement*, vol. 69, no. 10, pp. 8335–8343, 2020.

- [4] X. Yu, M. Z. Aziz, M. T. Sadiq, Z. Fan, and G. Xiao, "A new framework for automatic detection of motor and mental imagery EEG signals for robust bci systems," *IEEE Transactions on Instrumentation and Measurement*, vol. 70, pp. 1–12, 2021.
- [5] G. Fabiani, D. McFarland, J. Wolpaw, and G. Pfurtscheller, "Conversion of EEG activity into cursor movement by a brain-computer interface (BCI)," *IEEE Transactions on Neural Systems and Rehabilitation Engineering*, vol. 12, no. 3, pp. 331–338, 2004.
- [6] "Trends in EEG-BCI for daily-life: Requirements for artifact removal," *Biomedical Signal Processing and Control*, vol. 31, pp. 407–418, 2017.
- [7] J. Jin, Y. Miao, I. Daly, C. Zuo, D. Hu, and A. Cichocki, "Correlation-based channel selection and regularized feature optimization for MI-based BCI," *Neural Networks*, vol. 118, pp. 262–270, 2019.
- [8] M. A. Khan, R. Das, H. K. Iversen, and S. Puthusserypady, "Review on motor imagery based BCI systems for upper limb post-stroke neurorehabilitation: From designing to application," *Computers in Biology and Medicine*, vol. 123, p. 103843, 2020.
- [9] Z. Bai, K. Fong, J. J. Zhang, J. Chan, and K. Ting, "Immediate and long-term effects of BCI-based rehabilitation of the upper extremity after stroke: a systematic review and meta-analysis," *Journal of NeuroEngineering and Rehabilitation*, vol. 17, no. 1, pp. 57–76, 2020.
- [10] J. Cui, Z. Lan, O. Sourina, and W. Müller-Wittig, "EEG-based cross-subject driver drowsiness recognition with an interpretable convolutional neural network," *IEEE Transactions on Neural Networks and Learning Systems*, pp. 1–13, 2022.
- [11] E. V. Bobrova, V. V. Reshetnikova, A. A. Frolov, and Y. P. Gerasimenko, "Use of imaginary lower limb movements to control brain-computer interface systems," *Neuroscience and Behavioral Physiology*, vol. 50, no. 3, pp. 585–592, 2020.
- [12] J. Wang, W. Wang, S. Ren, W. Shi, and Z.-G. Hou, "Neural correlates of single-task versus cognitive-motor dual-task training," *IEEE Transactions on Cognitive and Developmental Systems*, vol. 14, no. 2, pp. 532–540, 2022.
- [13] Y.-T. Liu, Y.-Y. Lin, S.-L. Wu, C.-H. Chuang, and C.-T. Lin, "Brain dynamics in predicting driving fatigue using a recurrent self-evolving fuzzy neural network," *IEEE Transactions on Neural Networks and Learning Systems*, vol. 27, no. 2, pp. 347–360, 2016.
- [14] L. Angrisani, P. Arpaia, A. Esposito, and N. Moccaldi, "A wearable brain-computer interface instrument for augmented reality-based inspection in industry 4.0," *IEEE Transactions on Instrumentation and Measurement*, vol. 69, no. 4, pp. 1530–1539, 2020.
- [15] K. Värbu, N. Muhammad, and Y. Muhammad, "Past, present, and future of EEG-based BCI applications," *Sensors*, vol. 22, no. 9, p. 3331, 2022.
- [16] H. Lu, H. L. Eng, C. Guan, K. N. Plataniotis, and A. N. Venetsanopoulos, "Regularized common spatial pattern with aggregation for EEG classification in small-sample setting," *IEEE Transactions on Biomedical Engineering*, vol. 57, no. 12, pp. 2936–2946, 2010.
- [17] P. Gaur, H. Gupta, A. Chowdhury, K. McCreadie, R. B. Pachori, and H. Wang, "A sliding window common spatial pattern for enhancing motor imagery classification in EEG-BCI," *IEEE Transactions on Instrumentation and Measurement*, vol. 70, pp. 1–9, 2021.
- [18] J. Cui, Z. Lan, O. Sourina, and W. Müller-Wittig, "EEG-based cross-subject driver drowsiness recognition with an interpretable convolutional neural network," *IEEE Transactions on Neural Networks and Learning Systems*, pp. 1–13, 2022.
- [19] A. Liu, Q. Liu, X. Zhang, and X. Chen, "Muscle artifact removal toward mobile SSVEP-based BCI: A comparative study," *IEEE Transactions on Instrumentation and Measurement*, vol. 70, pp. 1–12, 2021.
- [20] J. Wang, L. Shi, W. Wang, and Z.-G. Hou, "Efficient brain decoding based on adaptive EEG channel selection and transformation," *IEEE Transactions on Emerging Topics in Computational Intelligence*, vol. 6, no. 6, pp. 1314–1323, 2022.
- [21] C. L. Baldwin and B. Penaranda, "Adaptive training using an artificial neural network and EEG metrics for within-and cross-task workload classification," *NeuroImage*, vol. 59, no. 1, pp. 48–56, 2012.
- [22] Y. Han, P. Ziebell, A. Riccio, and S. Halder, "Two sides of the same coin: adaptation of BCIs to internal states with user-centered design and electrophysiological features," *Brain-Computer Interfaces*, vol. 9, no. 2, pp. 102–114, 2022.
- [23] M. J. Antony, B. P. Sankaralingam, R. K. Mahendran, A. A. Gardezi, M. Shafiq, J.-G. Choi, and H. Hamam, "Classification of EEG using adaptive SVM classifier with CSP and online recursive independent component analysis," *Sensors*, vol. 22, no. 19, p. 7596, 2022.
- [24] P. Wang, P. Gong, Y. Zhou, X. Wen, and D. Zhang, "Decoding the continuous motion imagery trajectories of upper limb skeleton points for EEG-based brain-computer interface," *IEEE Transactions on Instrumentation and Measurement*, vol. 72, pp. 1–12, 2023.
- [25] K. Zhang, N. Robinson, S.-W. Lee, and C. Guan, "Adaptive transfer learning for EEG motor imagery classification with deep convolutional neural network," *Neural Networks*, vol. 136, pp. 1–10, 2021.
- [26] A. Eldenfria and H. Al-Samarraie, "Towards an online continuous adaptation mechanism (OCAM) for enhanced engagement: An EEG study," *International Journal of Human-Computer Interaction*, vol. 35, no. 20, pp. 1960–1974, 2019.
- [27] Z. Ma, J. Cheng, and D. Tao, "Online learning using projections onto shrinkage closed balls for adaptive brain-computer interface," *Pattern Recognition*, vol. 97, p. 107017, 2020.
- [28] H. Komijani, M. R. Parsaei, E. Khajeh, M. J. Golkar, and H. Zarrabi, "EEG classification using recurrent adaptive neuro-fuzzy network based on time-series prediction," *Neural Computing and Applications*, vol. 31, pp. 2551–2562, 2019.
- [29] Q. Jiang, Y. Zhang, G. Ge, and Z. Xie, "An adaptive CSP and clustering classification for online motor imagery EEG," *IEEE Access*, vol. 8, pp. 156 117–156 128, 2020.
- [30] C. M. Wong, Z. Wang, M. Nakanishi, B. Wang, A. Rosa, C. P. Chen, T.-P. Jung, and F. Wan, "Online adaptation boosts SSVEP-based BCI performance," *IEEE Transactions on Biomedical Engineering*, vol. 69, no. 6, pp. 2018–2028, 2021.
- [31] K.-J. Chiang, D. Emmanouilidou, H. Gamper, D. Johnston, M. Jalobeanu, E. Cutrell, A. Wilson, W. W. An, and I. Tashev, "A closed-loop adaptive brain-computer interface framework: Improving the classifier with the use of error-related potentials," in *2021 10th International IEEE/EMBS Conference on Neural Engineering (NER)*. IEEE, 2021, pp. 487–490.
- [32] F. Wang, Z. Xu, W. Zhang, S. Wu, Y. Zhang, and S. Coleman, "An adaptive control approach for intelligent wheelchair based on BCI combining with QoO," in *2020 International Joint Conference on Neural Networks (IJCNN)*, 2020, pp. 1–8.
- [33] Y. Jia, N. Xi, F. Wang, Y. Wang, and X. Li, "Controlling telerobotic operations adaptive to quality of teleoperator and task dexterity," in *2011 IEEE/RSJ International Conference on Intelligent Robots and Systems*, 2011, pp. 184–189.
- [34] J. Jiang, E. Yin, C. Wang, M. Xu, and D. Ming, "Incorporation of dynamic stopping strategy into the high-speed SSVEP-based BCIs," *Journal of Neural Engineering*, vol. 15, no. 4, p. 046025, 2018.
- [35] H. Rivera-Flor, D. Gurve, A. Floriano, D. Delisle-Rodriguez, R. Mello, and T. Bastos-Filho, "CCA-based compressive sensing for SSVEP-based brain-computer interfaces to command a robotic wheelchair," *IEEE Transactions on Instrumentation and Measurement*, vol. 71, pp. 1–10, 2022.
- [36] L. Xu, M. Xu, T.-P. Jung, and D. Ming, "Review of brain encoding and decoding mechanisms for EEG-based brain-computer interface," *Cognitive Neurodynamics*, vol. 15, pp. 569–584, 2021.
- [37] S. Guan, K. Zhao, and S. Yang, "Motor imagery EEG classification based on decision tree framework and Riemannian geometry," *Computational Intelligence and Neuroscience*, vol. 2019, 2019.
- [38] M. A. Bakhshali, M. Khademi, A. Ebrahimi-Moghadam, and S. Moghimi, "EEG signal classification of imagined speech based on riemannian distance of correntropy spectral density," *Biomedical Signal Processing and Control*, vol. 59, p. 101899, 2020.
- [39] M. Moakher, "A differential geometric approach to the geometric mean of symmetric positive-definite matrices," *SIAM Journal on Matrix Analysis and Applications*, vol. 26, no. 3, pp. 735–747, 2005.
- [40] D. Marshall, D. Coyle, S. Wilson, and M. Callaghan, "Games, gameplay, and BCI: the state of the art," *IEEE Transactions on Computational Intelligence and AI in Games*, vol. 5, no. 2, pp. 82–99, 2013.
- [41] J. Wang, W. Wang, Z.-G. Hou, W. Shi, X. Liang, S. Ren, L. Peng, and Y.-J. Zhou, "BCI and multimodal feedback based attention regulation for lower limb rehabilitation," in *2019 International Joint Conference on Neural Networks*, 2019, pp. 1–7.
- [42] J. Wang, W. Wang, and Z.-G. Hou, "Toward improving engagement in neural rehabilitation: Attention enhancement based on brain-computer interface and audiovisual feedback," *IEEE Transactions on Cognitive and Developmental Systems*, vol. 12, no. 4, pp. 787–796, 2019.
- [43] P. K. Parashiva and A. Vinod, "Improving direction decoding accuracy during online motor imagery based brain-computer interface using error-related potentials," *Biomedical Signal Processing and Control*, vol. 74, p. 103515, 2022.
- [44] T. Tao, Y. Jia, G. Xu, R. Liang, Q. Zhang, L. Chen, Y. Gao, R. Chen, X. Zheng, and Y. Yu, "Enhancement of motor imagery training efficiency by an online adaptive training paradigm integrated with error related potential," *Journal of Neural Engineering*, 2023.

- [45] M. Spüler, W. Rosenstiel, and M. Bogdan, "Online adaptation of a c-VEP brain-computer interface (BCI) based on error-related potentials and unsupervised learning," *PLoS ONE*, vol. 7, no. 12, p. e51077, 2012.
- [46] D. J. McFarland, L. M. McCane, S. V. David, and J. R. Wolpaw, "Spatial filter selection for EEG-based communication," *Electroencephalography and Clinical Neurophysiology*, vol. 103, no. 3, pp. 386–394, 1997.
- [47] K. J. Miller, G. Schalk, E. E. Fetz, M. den Nijs, J. G. Ojemann, and R. P. N. Rao, "Cortical activity during motor execution, motor imagery, and imagery-based online feedback," *Proceedings of the National Academy of Sciences*, vol. 107, no. 9, pp. 4430–4435, 2010.
- [48] G. Pfurtscheller and F. L. Da Silva, "Event-related EEG/MEG synchronization and desynchronization: basic principles," *Clinical neurophysiology*, vol. 110, no. 11, pp. 1842–1857, 1999.
- [49] P. Suffczynski, S. Kalitzin, G. Pfurtscheller, and F. L. Da Silva, "Computational model of thalamo-cortical networks: Dynamical control of alpha rhythms in relation to focal attention," *International Journal of Psychophysiology*, vol. 43, no. 1, pp. 25–40, 2001.
- [50] J. Asensio-Cubero, J. Q. Gan, and R. Palaniappan, "Extracting optimal tempo-spatial features using local discriminant bases and common spatial patterns for brain computer interfacing," *Biomedical Signal Processing and Control*, vol. 8, no. 6, pp. 772–778, 2013.
- [51] J. Asensio-Cubero, J. Gan, and R. Palaniappan, "Multiresolution analysis over simple graphs for brain computer interfaces," *Journal of neural engineering*, vol. 10, no. 4, p. 046014, 2013.
- [52] K. K. Ang, Z. Y. Chin, H. Zhang, and C. Guan, "Filter bank common spatial pattern (FBCSP) in brain-computer interface," in *IEEE international joint conference on neural networks*. IEEE, 2008, pp. 2390–2397.
- [53] V. J. Lawhern, A. J. Solon, N. R. Waytowich, S. M. Gordon, C. P. Hung, and B. J. Lance, "EEGNet: a compact convolutional neural network for eeg-based brain-computer interfaces," *Journal of neural engineering*, vol. 15, no. 5, p. 056013, 2018.
- [54] R. T. Schirrmester, J. T. Springenberg, L. D. J. Fiederer, M. Glasstetter, K. Eggersperger, M. Tangermann, F. Hutter, W. Burgard, and T. Ball, "Deep learning with convolutional neural networks for EEG decoding and visualization," *Human brain mapping*, vol. 38, no. 11, pp. 5391–5420, 2017.
- [55] X. Jia, Y. Song, L. Yang, and L. Xie, "Joint spatial and temporal features extraction for multi-classification of motor imagery EEG," *Biomedical Signal Processing and Control*, vol. 71, p. 103247, 2022.
- [56] P. Auththasan, R. Chaisaen, T. Sudhawiyangkul, P. Rangpong, S. Kitathaveephong, N. Dilokthanakul, G. Bhakdisongkhram, H. Phan, C. Guan, and T. Wilaiprasitporn, "MIN2Net: End-to-end multi-task learning for subject-independent motor imagery EEG classification," *IEEE Transactions on Biomedical Engineering*, vol. 69, no. 6, pp. 2105–2118, 2021.



Weiqun Wang received the B.S. degree in mechanical engineering from Yanshan University, Qinhuangdao, China, in 2002, the M.S. degree in control theory and control engineering from Beijing Research Institute of Automation for Machinery Industry (BRIAMI), Beijing, China, in 2006, and the Ph.D. degree in control theory and control engineering from the Institute of Automation, Chinese Academy of Sciences (IACAS), Beijing, China, in 2014. From 2006 to 2011, he was an Electrical Engineer with the BRIAMI.

He is currently an Professor with the State Key Laboratory of Multimodal Artificial Intelligence Systems, IACAS. His current research interests include rehabilitation robotics, dynamic identification, interaction control, and optimization algorithms.



Jianqiang Su received his Bachelor of Engineering degree from Xi'an Jiaotong University in 2020. He is currently pursuing the Ph.D. degree in control science and engineering with the State Key Laboratory of Multimodal Artificial Intelligence Systems, Institute of Automation, Chinese Academy of Sciences, Beijing, China.

His current research interests include brain-computer interface, rehabilitation robot control, and signal processing.



Yihan Wang received his Bachelor of Engineering degree from University of Electronic Science and Technology of China in 2021. He is currently pursuing the Ph.D. degree in control science and engineering with the State Key Laboratory of Multimodal Artificial Intelligence Systems, Institute of Automation, Chinese Academy of Sciences, Beijing, China.

His current research interests include artificial intelligence, brain-computer interface, and neurorehabilitation.



Zeng-Guang Hou (F'18) received the B.E. and M.E. degrees in electrical engineering from Yanshan University, Qinhuangdao, China, in 1991 and 1993, respectively, and the Ph.D. degree in electrical engineering from the Beijing Institute of Technology, Beijing, China, in 1997.

From 1997 to 1999, he was a Post-Doctoral Research Fellow with the Key Laboratory of Systems and Control, Institute of Systems Science, Chinese Academy of Sciences (CAS), Beijing. He was a Research Assistant at the Hong Kong Polytechnic University, Hong Kong, from 2000 to 2001. From 2003 to 2004, he was a Visiting Professor at the Intelligent Systems Research Laboratory, College of Engineering, University of Saskatchewan, Saskatoon, SK, Canada. He is currently a Professor of the State Key Laboratory of Multimodal Artificial Intelligence Systems, Institute of Automation, CAS. His current research interests include computational intelligence, robotics, and intelligent systems.



Jiaying Wang received the B.E. degree in automation from the Central South University, Changsha, China, in 2016, and the Ph.D degree in control science and engineering from the Institute of Automation, Chinese Academy of Sciences, Beijing, China, in 2021.

She is currently working as an Assistant Professor at the Institute of Automation, Chinese Academy of Sciences, Beijing, China. Her research interests include brain-computer interface, rehabilitation robot control, and signal processing.